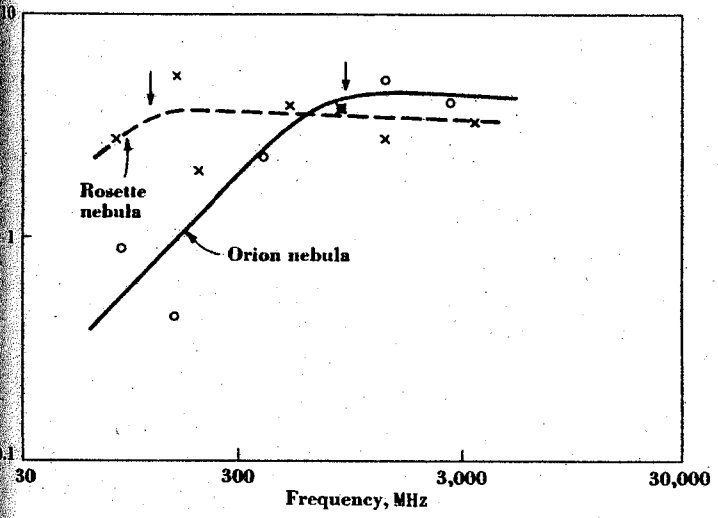

Fig. 8-56. Spectra of the Orion and Rosette nebulas. The circles are measured values for the Orion nebula, and the crosses are measured values for the Rosette nebula. The arrows indicate the peak frequencies of the spectra. (*After Menon*, 1962, 1964.)

for the Orion nebula. Upper limits for the ages of the nebulas have been placed at 10,000 years for the Orion nebula and 50,000 years for the Rosette nebula (Menon, 1964). These ages refer to the length of time during which ultraviolet excitation from the exciting (early-type) stellar sources has been important. As a result of the excitation, mass motions take place in the nebula which are believed to result in the irregular electron-density distributions found, for example, in the Rosette nebula.

Since the first measurements of ionized-hydrogen clouds by Haddock, Mayer, and Sloanaker (1954) a total of several dozen sources have been identified with such clouds. (Krymkin, 1978; Abramenko and Krymkin, 1982, 1983). Data on several of these sources, including the Orion and Rosette nebulas, are summarized in Table 8-5.

8-24 Line-Emission Clouds and Galactic Structure Observations of the continuum radiation of thermal and nonthermal radio sources of the type we have been discussing are usually conducted using receivers of wide bandwidth, with the exact frequency of operation being noncritical. This continuum radiation extends over essentially all frequencies with varying intensity, the emission coming from nonresonant processes. In contrast to this broadband continuum radiation there is also narrow-band emission, or absorption, related to the difference in energy levels of atoms or molecules. Observations of these

Table 8-5
Galactic thermal sources (H II regions)

Object	*Flux density, Jy**	*Distance, pc*
Cygnus X	~5,000	~1,000
Omega nebula (M 17)	1,000	1,700
North America nebula	550	900
Orion nebula (M 42)	520	500
Rosette nebula	260	1,400
Lagoon nebula (M 8)	260	1,200

* At 1.4 GHz

spectral lines are made with narrowband receivers, with the exact frequency of observation being of prime importance.

The possibility of a spectral line from neutral interstellar hydrogen at 1,420 MHz (21 cm) was reported by van de Hulst (1945) of Leiden, Netherlands, in 1945.† The line was detected in emission in 1951 by Ewen and Purcell (1951) at Harvard and a few weeks later by groups in the Netherlands and in Australia. The line was detected in absorption in 1954 by Hagen and McClain (1954) at the U.S. Naval Research Laboratory. Although attempts were made to detect other atomic or molecular lines, such as the 327-MHz line of deuterium and the 1,665- and 1,667-MHz lines of the OH radical, all were unsuccessful until 1963, when Weinreb, Barrett, Meeks, and Henry (1963) detected the close pair of OH ($O^{16}H^{1}$) lines in absorption. They noted the decrease in intensity of Cassiopeia A at or close to the OH-line frequencies caused by absorption of OH over the path between the earth and Cassiopeia A. Absorption by neutral hydrogen over the same path had been observed by Hagen and McClain in 1954.

The neutral-hydrogen (H I) transition is associated with a transition between two closely-spaced energy levels of the ground state related to the electron spin, or magnetic dipole orientation. When the magnetic dipole moment of the electron is parallel to that of the nucleus, the energy of the hydrogen atom is very slightly greater than when the dipole moments are opposed. The transition between these two substates is called a *hyperfine transition*. The probability of spontaneous emission is so low that an atom in the higher state remains there for 11 million years, on the average, before falling to the lower state, with the emission of a 21-cm photon. This low probability and the lack of knowledge of the density of neutral hydrogen in interstellar space made it quite uncertain whether the line could be detected. However, the

† More historical background on this is given in Chapter 1.

Fig. 8-57. Hendrick van de Hulst who suggested searching for the 21 cm line of neutral hydrogen and pioneered in using line observations to determine the structure of our galaxy.

suggestion by van de Hulst (Fig. 8-57) that a search be made brought positive results 6 years later.

Observations of the 21-cm hydrogen line have enabled radio astronomers to deduce for the first time a picture of the spiral structure of our galaxy. From profiles of intensity vs. frequency (or radial velocity) it is found that in some directions the neutral hydrogen is moving toward us and in other directions away from us, with velocities up to several hundred kilometers per second. From such observations around the galactic plane and a suitable velocity-distance model, it is possible to construct an approximate map of the distribution of neutral hydrogen in our galaxy. Such a picture assembled from Dutch and Australian observations is presented in Fig. 8-58 (Kerr and Westerhout, 1964). The positions of the sun and galactic nucleus are shown. Their distance of separation is about 30,000 light-years. In directions near the galactic center the radial velocity due to galactic rotation tends to approach zero and to become confused with radial velocities due to local turbulences. Hence, a sector toward the galactic center is left blank in Fig. 8-58. In spite of this problem, observations of the galactic nucleus (Sagittarius A) at the hydrogen line and also in the continuum indicate the existence of a remarkable structure at the center of our galaxy (Rougoor and Oort, 1960). There appears to be a small source at the center of a flat disk and a ring of neutral hydrogen, with all three components (source, disk, and ring) embedded in a nonthermal source produced

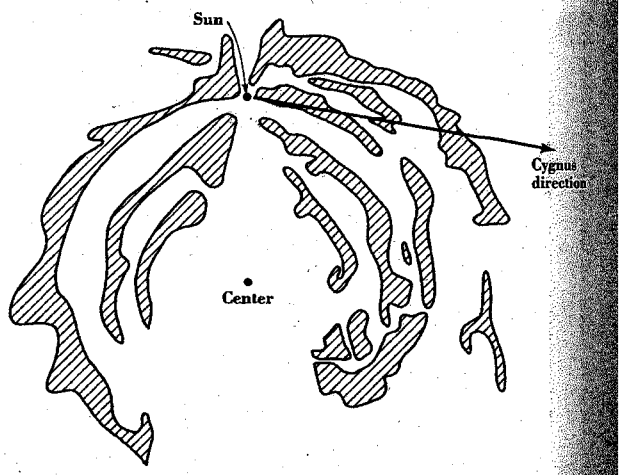

Fig. 8-58. Distribution of neutral hydrogen in our galaxy, showing its complex spiral structure. Shaded areas correspond to the regions of greatest neutral hydrogen concentration as deduced from 21-cm observations. (*After Kerr and Westerhout*, 1964.)

by relativistic electrons moving in a magnetic field. Regions near the center show both high rotational velocity and rapid expansion radially outward. The reasons for this complex structure are not known, but some astronomers suggest that the structure is the result of an explosion in the nucleus in an earlier epoch (Westerhout, 1964). A further discussion of the galactic nucleus is given in Sec. 8-27.

The profile (intensity vs. frequency) obtained when a stationary region of neutral hydrogen is scanned in frequency with a narrow-band receiver is as suggested in Fig. 8-59*a*. The profile is centered on 1,420 MHz, and its width is a measure of the receiver bandpass characteristics. It is assumed that the neutral-hydrogen cloud is stationary (with respect to the observer) and has no internal turbulence or thermal broadening. If the cloud has no internal turbulence or thermal broadening but is moving as a whole away from the observer, the profile of Fig. 8-59*a* would be displaced down in frequency, as suggested in Fig. 8-59*b*, where the frequency shift $\Delta\nu$ is related to the velocity of recession v by

$$\mp v = c\,\frac{\pm\Delta\nu}{\nu} \tag{8-47}$$

where v = velocity of approach (−) or recession (+)
c = velocity of light

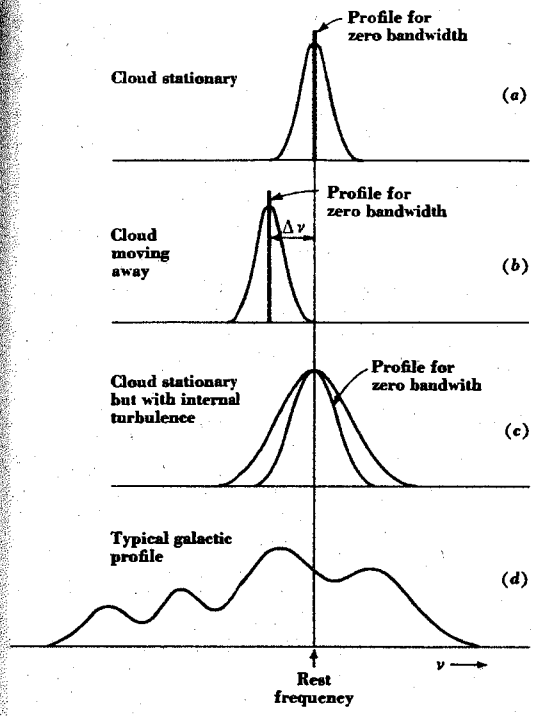

Fig. 8-59. Idealized hydrogen-line profiles.

$\Delta\nu$ = frequency shift

ν = rest frequency (= 1,420 MHz)

At the hydrogen-line frequency, a shift of 5 kHz corresponds to a velocity of 1.056 km sec^{-1}. Equation (8-47) is a simplification of a more general relation and holds only for $v \ll c$. If the receiver had a frequency response approaching zero bandwidth, the profiles in Fig. 8-59*a* and *b* would be delta functions, as indicated.

If the cloud is stationary as a whole with respect to the observer but has thermal broadening and/or turbulence of a symmetrical type, then the profile will be broadened, but the peak will not be displaced, as suggested in Fig. 8-59*c*. A broadened profile would also be obtained with a zero-bandwidth receiver, but the profile would be less broad. The zero-bandwidth profile is the true profile, which may be approached but not attained in practice as the bandwidth is reduced. The observed profile is the convolution of this true profile and the receiver profile.

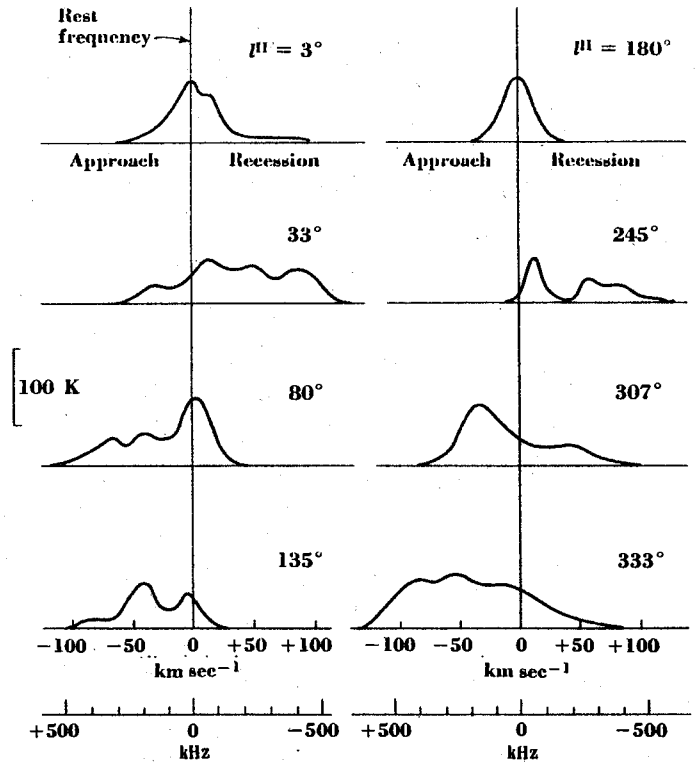

Fig. 8-60. Hydrogen-line profiles at different longitudes in the plane of our galaxy. (*After Kerr and Westerhout*, 1964).

In general, in measurements of galactic hydrogen, the gas may be in relative motion with respect to the observer and also have internal motions. The profile of Fig. 8-59*d* is typical. It suggests that there are four regions, or clouds, in the direction of the antenna beam, with three clouds receding from the observer at different velocities and one cloud approaching. All four peaks are broadened, suggesting also that the clouds have internal motions.

In the measurements of the neutral-hydrogen radiation from our galaxy, profiles were obtained along the equator at different galactic longitudes, of which those in Fig. 8-60 are typical (Kerr and Westerhout, 1964). Referring to Fig. 8-60 and to the sketch of Fig. 8-61, showing the coordinates in the galactic plane, we note that in a direction close to the center of the galaxy (l^{II} = 3°) the peak is centered on the rest frequency (1,420 MHz), indicating no relative motion. In the direction l^{II} = 33° the profile is displaced to the right,

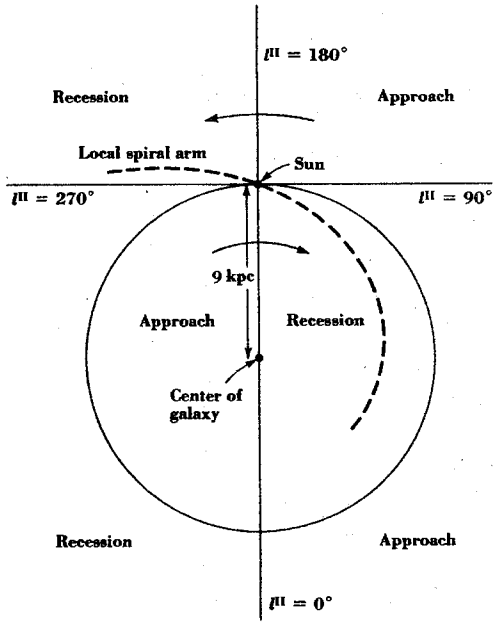

Fig. 8-61. Simplified plan-view sketch of our galaxy showing regions of relative approach and recession with respect to the sun. The local spiral arm is indicated by the dashed line.

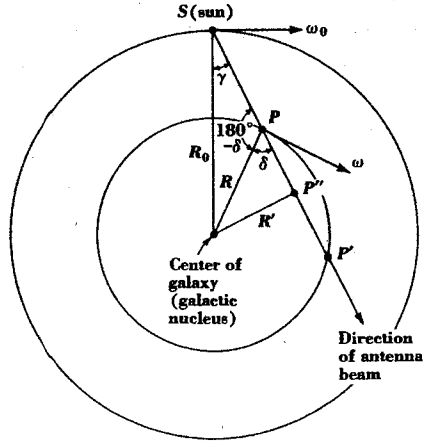

Fig. 8-62. Simplified model of galactic motions with associated geometry.

indicating recession. According to Fig. 8-61, this would be expected if the emission is from regions inside of a circle having the galactic nucleus-sun distance as radius. Assuming the sun to be stationary, motion inside the circle would be clockwise, as indicated, on the assumption that the galaxy is winding up (note hypothetical path of spiral arm through sun shown by dashed line). In the directions $l^{II} = 80$ and 135° the profiles show approach, while at 180°, in the direction of the galactic anticenter, there is no relative motion. At $l^{II} = 245°$ the profile indicates recession, but the profiles at 307 and 333° show approach.

The peaks in the profiles of Fig. 8-60 can be interpreted as related to different spiral arms. A detailed interpretation, however, requires that a model be assumed for the galactic motions. Such a simple, idealized model is shown in Fig. 8-62. It is assumed that the galactic motions are circular and that the angular velocity ω is constant at any radius R. As shown by van de Hulst, Muller, and Oort (1954), the relative velocity v of the point P with respect to S (the sun) is given by

$$v = \omega R \sin \delta - \omega_0 R_0 \sin \gamma \tag{8-48}$$

where ω_0 = angular velocity at sun's radius
R_0 = sun's radius from center of galaxy
γ = angle between antenna beam and galactic nucleus
δ = angle at point P between antenna beam and galactic nucleus

From the theorem of sines

$$\frac{\sin \gamma}{R} = \frac{\sin (180° - \delta)}{R_0} = \frac{\sin \delta}{R_0} \tag{8-49}$$

or

$$R \sin \delta = R_0 \sin \gamma \tag{8-50}$$

From (8-50) and (8-48) we then obtain

$$v = (\omega - \omega_0) R_0 \sin \gamma \tag{8-51}$$

In (8-51) v can be calculated by (8-47) from the observed hydrogen-line displacement, γ is known from the antenna setting, and ω_0 and R_0 are given by the galactic model. The angular velocity ω of the hydrogen region at the point P can then be calculated from (8-51). From a known or assumed relation between ω and R, the radius R of the point P can be determined and, hence, the distance SP. Knowing the distance SP, the direction γ, and the flux density, a map of the neutral-hydrogen distribution, such as Fig. 8-58, can be constructed.

The above discussion is somewhat oversimplified. Thus, the sun's motion in the solar neighborhood makes it desirable to refer the motions to the local standard of rest (see Chap. 2) instead of to the sun. The motion of the observer

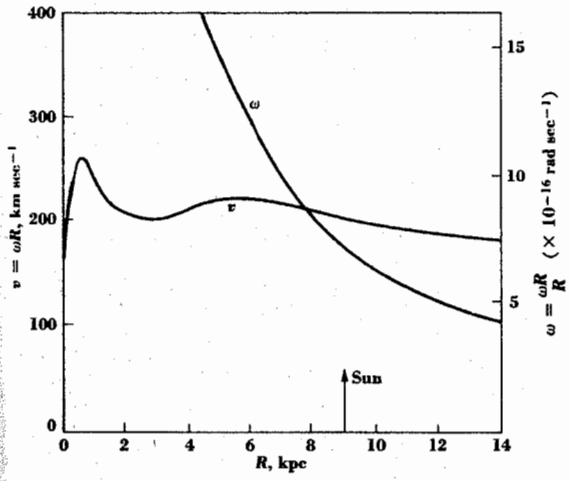

Fig. 8-63. Circular velocity v and angular velocity ω in our galaxy as a function of distance R from the center. (*After Rougoor and Oort*, 1960.)

on the earth with respect to this local standard of rest also needs to be taken into account. Furthermore, referring to Fig. 8-62, it is evident that there will be an ambiguity in the distance determination, since for a given ω and R the hydrogen-line region could be either at P or P'. However, if the largest radial velocity in the line profile is taken, it should correspond without ambiguity to the point P'' at a radius R'. Outside of the radius R_0 the position ambiguity does not occur. A graph of $v = \omega R$ versus R from Rougoor and Oort (1960) is shown in Fig. 8-63, along with a curve of ω versus R. It is the latter curve that is useful in converting ω to R.

The above discussion has been concerned with line emission. Let us analyze next the problem of *line absorption* (Purcell and Ewen, 1951; van de Hulst, Muller, and Oort, 1954; Hagen, Lilley, and McClain, 1955). Suppose that a homogeneous line cloud filling the antenna beam is located between the observer and a discrete source, as in Fig. 8-64. If T_s' is the observed antenna temperature due to the source in the continuum immediately adjacent to the line, then in the cloud's line frequency range (signal band) the antenna temperature is given by (see (3-104))

$$T_l = T_s' e^{-\tau} + T_c' (1 - e^{-\tau}) \tag{8-52}$$

where T_l = signal band or line temperature
τ = optical depth of cloud in the line ($\tau = f(\nu)$)
T_s' = apparent source temperature, or antenna temperature due to source ($= T_s \Omega_s / \Omega_A$; $\Omega_s \ll \Omega_A$)

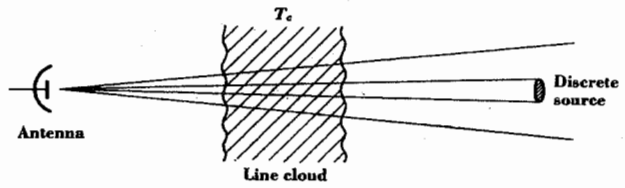

Fig. 8-64. Line cloud (hydrogen line or other atomic or molecular line) and discrete source in antenna beam of radio telescope.

T_c' = apparent cloud temperature, or antenna temperature due to cloud in the line ($= T_c \Omega_M / \Omega_A$)
T_s = true source temperature
T_c = true cloud temperature in the line
Ω_s = source solid angle
Ω_A = antenna beam solid angle
Ω_M = main beam solid angle

The first term in (8-52) involves line absorption, while the second term involves both line emission and absorption. For frequencies just removed from the line (comparison band) $\tau = 0$, and we have

$$T = T_s' \tag{8-53}$$

where T = comparison-band temperature (off of line)
It is assumed that the source temperature is substantially constant across both bands (signal and comparison). By arranging the radiometer to measure the difference of the signal and comparison bands ($T_l - T = \Delta T$) the radiometer (on-source) output is

$$\Delta T = T_s' e^{-\tau} + T_c' (1 - e^{-\tau}) - T_s' \tag{8-54}$$

or

$$\Delta T = (T_c' - T_s')(1 - e^{-\tau}) \tag{8-55}$$

Three cases are of interest:

(1) If $T_c' > T_s'$ (apparent cloud line temperature greater than apparent source temperature), the difference ΔT is positive, and the line is seen in *emission*.
(2) If $T_c' = T_s'$, the output is zero.
(3) If $T_c' < T_s'$, the difference ΔT is negative, and the line is seen in *absorption*.

If the antenna beam is moved off the discrete source but is still filled by the cloud, we have, assuming a negligible change in cloud effect, that the radiometer (off-source) output is

$$\Delta T' = T_c'(1 - e^{-\tau}) \tag{8-56}$$

Equation (8-56) describes the situation for a simple emission measurement, while (8-55) describes the situation for an absorption measurement making use of a discrete source. If the optical depth of the cloud is small ($\tau \ll 1$), we have approximately that

$$\Delta T' = T_c' \tau \quad \text{off source} \tag{8-57}$$

and

$$\Delta T = (T_c' - T_s')\tau \quad \text{on source} \tag{8-58}$$

From (8-57) and (8-58) it is clear that if $T_s' \gg T_c'$, the line will be much more readily detected in absorption than in emission. The requirement $T_s' \gg T_c'$ can usually be met by using a sufficiently directive antenna and/or selecting a sufficiently strong discrete source. Subtracting (8-56) from (8-55) gives

$$\Delta T - \Delta T' = -T_s'(1 - e^{-\tau}) \tag{8-59}$$

from which

$$\tau = -\ln\left(\frac{\Delta T - \Delta T'}{T_s'} + 1\right) \tag{8-60}$$

From (8-56) and (8-59) we also have that the cloud temperature

$$T_c = \frac{T_s' \Delta T' \Omega_A}{(\Delta T' - \Delta T)\Omega_M} \tag{8-61}$$

where ΔT = radiometer output on source
$\Delta T'$ = radiometer output off source
T_s' = apparent source temperature
Ω_M = main beam solid angle
Ω_A = beam solid angle

Thus, from measurements of T_s', ΔT, and $\Delta T'$ and a knowledge of the antenna beam angles the optical depth τ and line temperature T_c of the cloud can be deduced. The above relations apply to a homogeneous cloud between the source and observer which fills the antenna (main) beam.

If there are several line clouds in the antenna beam, the above analysis requires revision. Following Hagen, Lilley, and McClain (1955), consider the case of two line clouds i and j in the antenna beam subtending solid angles Ω_i and Ω_j, respectively, as in Fig. 8-65. Let the i-cloud optical depth be τ_i and the j-cloud optical depth be τ_j. Assuming further that the i cloud is in line with the

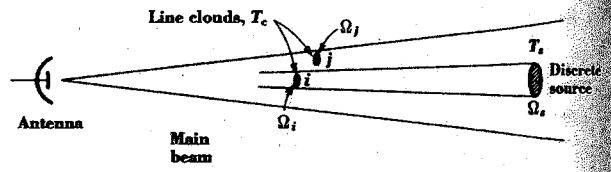

Fig. 8-65. Several line clouds and discrete source in antenna beam of radio telescope.

discrete source and that the antenna beam is aligned with both, the signal band gives

$$T_l = T_s \frac{\Omega_s - \Omega_i}{\Omega_A} + T_s \frac{\Omega_i}{\Omega_A} e^{-\tau_i} + T_c(1 - e^{-\tau_i}) \frac{\Omega_i}{\Omega_A} + T_c(1 - e^{-\tau_i}) \frac{\Omega_j}{\Omega_A} P_{nj} \tag{8-62}$$

and the comparison band yields

$$T = T_s \frac{\Omega_s}{\Omega_A} \tag{8-63}$$

where T_s = source temperature (assumed uniform)
T_c = cloud line temperature (assumed uniform)
Ω_s = source solid angle
Ω_i = i-cloud solid angle
Ω_j = j-cloud solid angle
Ω_A = beam solid angle
τ_i = optical depth of i cloud
τ_j = optical depth of j cloud
P_{nj} = normalized antenna-power-pattern value in direction of j cloud

The first term in (8-62) gives the temperature contribution due to the part of the source not shielded by the i cloud, it being assumed that $\Omega_i < \Omega_s$. The second term is equal to the contribution from the shielded part of the source as affected by absorption in the i cloud. The third and fourth terms give the temperature contributions due to emission and internal absorption from the i and j clouds, respectively. Subtracting T from T_l yields the radiometer (on-source) output

$$\Delta T = \left(T_c \frac{\Omega_i}{\Omega_A} - T_s' \frac{\Omega_i}{\Omega_s}\right)(1 - e^{-\tau_i}) + T_c(1 - e^{-\tau_i}) \frac{\Omega_j}{\Omega_A} P_{nj} \tag{8-64}$$

where T_s' = apparent or antenna temperature due to source $[= T_s \Omega_s / \Omega_A]$

Note that $T_s' \frac{\Omega_i}{\Omega_s} = T_s \frac{\Omega_s}{\Omega_A} \frac{\Omega_i}{\Omega_s} = T_s \frac{\Omega_i}{\Omega_A}$

For a number of line clouds (more than the two assumed above) the radiometer (on source) output would be given by summing terms like the first one in (8-64) over all i clouds (in cone subtended by the discrete source) and summing terms like the second one over all j clouds (in antenna beam but not in cone subtended by the discrete source). Rearranging yields

$$\Delta T = -\sum_i T_s'(1-e^{-\tau_i}) \frac{\Omega_i}{\Omega_s} + \sum_{i,j} T_c(1-e^{-\tau_{i,j}}) \frac{\Omega_{i,j}}{\Omega_A} P_{ni,j} \tag{8-65}$$

In (8-65) the first term is taken over all i clouds and gives the contribution due to the absorption of the source continuum radiation produced by the i clouds. The second term is taken over all clouds (i and j) and represents the contribution due to the line emission from all line clouds in the antenna beam. The latter may be replaced by the mean $\overline{\Delta T'}$ of the line profiles in nearby comparison regions (beam off source) assuming that the comparison regions differ but little from the on-source region. Further, if $\Omega_i \simeq \Omega_s$, (8-65) reduces to

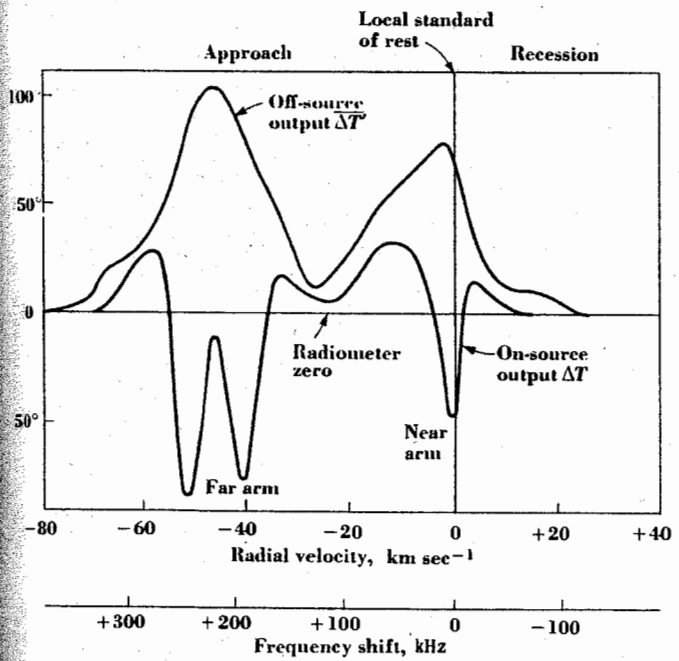

Fig. 8-66. Hydrogen-line emission profiles near Cassiopeia A (upper) and absorption profile in the direction of Cassiopeia A (lower). The ordinate is output temperature in kelvins. (*After Hagen, Lilley, and McClain*, 1955.)

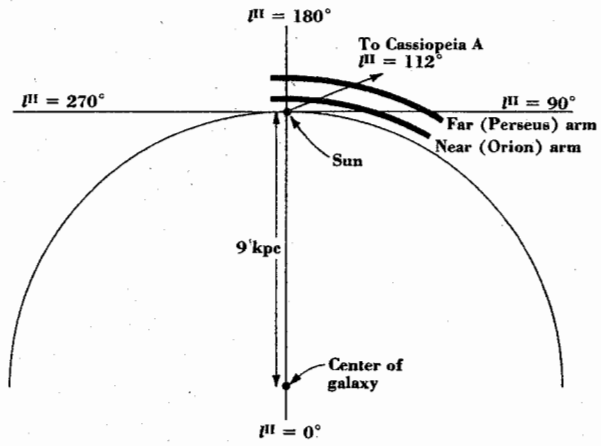

Fig. 8-67. Galactic structure in the direction of Cassiopeia A.

$$\Delta T = -T_s'(1-e^{-\tau_l}) + \overline{\Delta T'} \tag{8-66}$$

where τ_l = total optical depth of all line clouds between observer and discrete source (within Ω_s)

From (8-66)

$$\tau_l = -\ln\left(\frac{\Delta T - \overline{\Delta T'}}{T_s'} + 1\right) \tag{8-67}$$

where ΔT = radiometer on-source output
$\overline{\Delta T'}$ = mean radiometer off-source output
T_s' = apparent or antenna temperature due to discrete source

In neutral-hydrogen measurements in the direction of the discrete source Cassiopeia A, Hagen, Lilley, and McClain (1955) obtained the profiles shown in Fig. 8-66. The on-source (signal-band) output ΔT exhibits three well-defined absorption minima. The pair with the larger frequency displacement is interpreted as being due to two neutral-hydrogen clouds in the far arm of the local galactic structure, while the third absorption minimum is believed due to a cloud in the near arm. Cassiopeia A is situated beyond the second arm, as suggested in Fig. 8-67. From their measurements (Hagen et al., 1955) the data of Table 8-6 were obtained. A size estimate for the clouds may be deduced from the fact that a cloud in the far arm which just covers Cassiopeia A (angular diameter 6 min of arc) would be about 5 pc in diameter.

Table 8-6

Object	*Radial velocity km sec*$^{-1}$	$\lvert\overline{\Delta T'} - \Delta T\rvert$, *K*	*Optical depth,* τ_l*(max)*
Near-arm cloud (Orion)	−1.0	71.5	0.96
Far-arm cloud I (Perseus)	−38.5	89.4	1.47
Far-arm cloud II (Perseus)	−48.6	100	2.04

The total number of hydrogen atoms N_l in a column of 1-m^2 cross-section is given by

$$N_l = 1.835 \times 10^{22} T \int \tau(v)\ dv \qquad (8\text{-}68)$$

where T = cloud kinetic temperature, K
$\tau(v)$ = optical depth as a function of velocity
dv = elemental velocity, km sec^{-1}

The integration is carried out over the velocity range of a given hydrogen-line feature to obtain the number of atoms it contains. According to Hagen, Lilley and McClain, the total number of neutral hydrogen atoms per square meter in the near-arm cloud is about 2×10^{25}. If the cloud is 5 pc thick, the density is about 130 cm^{-3}.†

The lower (absorption) curve in Fig. 8-66 has much sharper features than the upper (emission) curve because the angular diameter of the discrete source (Cassiopeia A) is much less than the beam width of the 15 m antenna used by Hagen, Lilley, and McClain. The diameter of Cassiopeia A is about 5 min of arc, while the half-power beam width of the 15 m antenna at 1,420 MHz is about 50 min of arc, or 10 times as great. To achieve the same resolution in emission would require a 150 m-diameter antenna. The selection of a still smaller discrete source could yield even sharper absorption profiles.

From observations of hydrogen-line absorption in the direction of a number of intense radio sources, Clark (1965) concludes that there are, on the average, about four neutral-hydrogen clouds per kiloparsec in the galactic plane, with perhaps a higher density in the local spiral arm.

† By way of comparison, the density of neutral hydrogen is about 1 cm^{-3} in the interstellar medium of the solar neighborhood. On the other hand, the (ionized) hydrogen density in the Orion nebula is ~1,000 cm^{-3}.

8-25 Interstellar Molecular Lines Following the suggestion by I. S. Shklovsky (1953), the first attempt at the detection of a molecular line (OH) was made by Barrett and Lilley (1957). It was unsuccessful because the line frequencies were not known with sufficient accuracy at that time. But after they had been measured in the laboratory, Weinreb, Barrett, Meeks and Henry (1963) made a new attempt and detected OH in the absorption spectrum of Cassiopeia A during the first hours of their observations.

Since then the field of molecular radio astronomy has mushroomed and the interstellar medium found to be a veritable soup of diverse molecular species, some in giant clouds of 10^6 solar masses with densities of 10^3 to 10^6 cm^{-3}. A good historical summary is given by Barrett (1983). The role of the interstellar molecular clouds in the formation of stellar systems is explained by Gehrz, Black and Solomon (1984).

The study of radio molecules has also extended to circumstellar envelopes of evolved, oxygen-rich giant stars where ground state OH maser data have provided important information regarding the envelope structure and dynamics (Davis, Seaquist and Purton, 1979). And with observations of excited rotational states of OH, information can be gleaned regarding OH abundance and excitation. This has been done, for example, by the detection of the 6035 MHz OH line toward the compact nebula Vyssotsky 2-2, believed to be an evolved red giant in transition to a planetary nebula (Jewell, Schenwerk and Snyder, 1985).

The OH line involves an electric dipole transition which is much more intense than the magnetic dipole transition of the hydrogen line. The OH transition probability is also higher. As a result, it has been possible to detect the OH line even though the OH abundance appears generally to be very much less than that of neutral hydrogen. Over the Cassiopeia A path the neutral hydrogen atoms are 20 million times more abundant than the OH radicals (Barrett, 1964). Australian observers (Robinson et al., 1964) indicate that in the direction of the galactic nucleus this ratio is much smaller (relatively more OH). They also find curious concentrations of OH near the nucleus that differ significantly in radial-velocity distribution from the neutral-hydrogen concentrations. The Australian group (Gardner, Robinson, Bolton, and van Damme, 1964) has also detected the two OH satellite lines at 1,612 and 1,720 MHz. These lines are not so strong as the close pair at 1,665 and 1,667 MHz.

A level diagram for the OH transitions is shown in Fig. 8-68. For thermodynamic equilibrium and the medium only weakly absorbing, line-intensities should be in the ratio 1:5:9:1 (1612, 1665, 1667, 1720 MHz). If the medium is strongly absorbing, the line-intensity ratios should approach unity (Barrett, 1967). In the event of maser action, line-intensity ratios may be modified due to amplification. For this to occur, the population of the higher energy levels of the radio lines must exceed the population of the lower energy